SUPPORTING INFORMATION for:

Ion-Dipole-Interaction-Driven Complexation of Polyethers with Polyviologen-Based Single-Ion Conductors

Minjae Lee,[1] Harry W. Gibson,[2] Taehoon Kim,[3] Ralph H. Colby,[4] U Hyeok Choi[*5]

[1] Department of Chemistry, Kunsan National University, Gunsan 55150, Korea

[2] Department of Chemistry, Virginia Polytechnic Institute and State University, Blacksburg, Virginia 24061, United States

[3] Functional Composite Department, Korea Institute of Materials Science (KIMS), Changwon 51508, Korea

[4] Department of Materials Science and Engineering, Pennsylvania State University, University Park, Pennsylvania 16802, United States

[5] Department of Polymer Engineering, Pukyong National University, Busan 48547, Korea

*Corresponding Author E-mail: uhyeok@pknu.ac.kr

Contents

PV_C_{10}

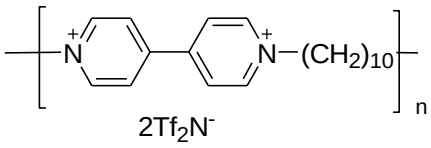

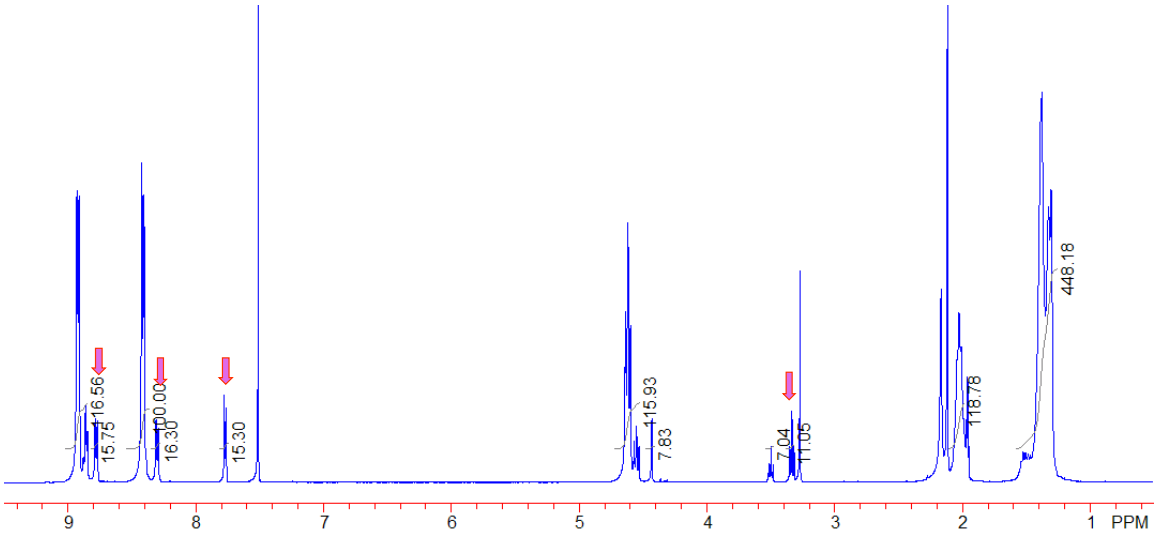

Figure S1. ^{1}H NMR spectrum of PV_C_{10} (400 MHz, $CD_3CN/CDCl_3$ 2:3 (v/v), 23 ℃). The end-group protons are shown as the arrows.

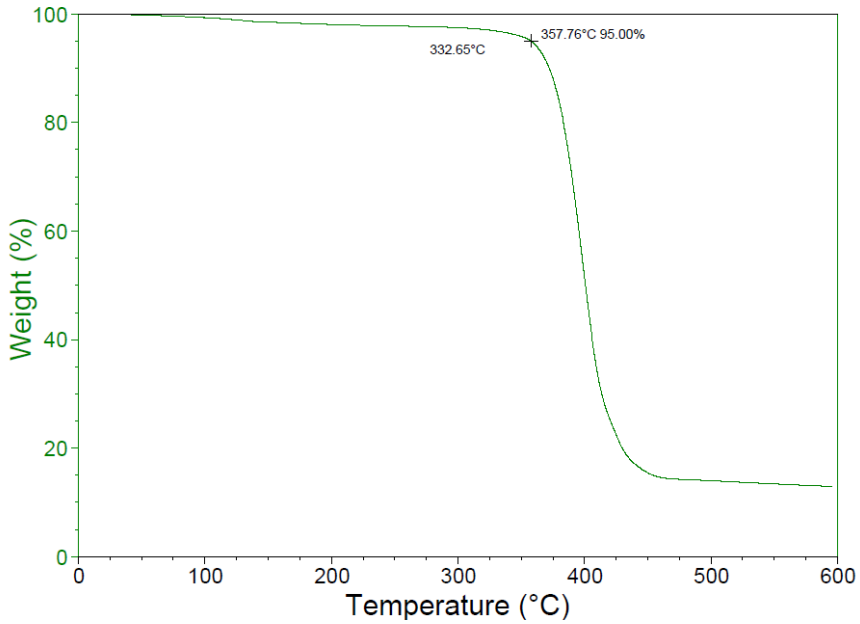

Figure S2. TGA thermogram of PV_C_{10}.

PV_C_6/C_{10}

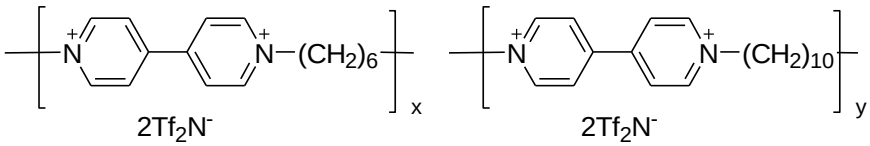

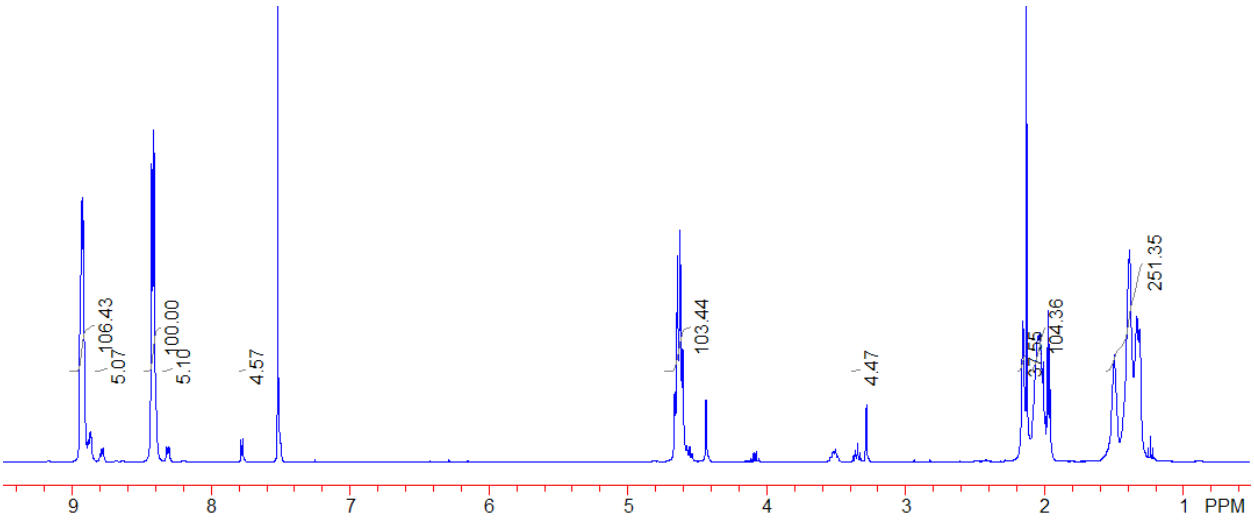

Figure S3. ^{1}H NMR spectrum of PV_C_6/C_{10} (400 MHz, CD_3CN/$CDCl_3$ 2:3 (v/v), 23 °C).

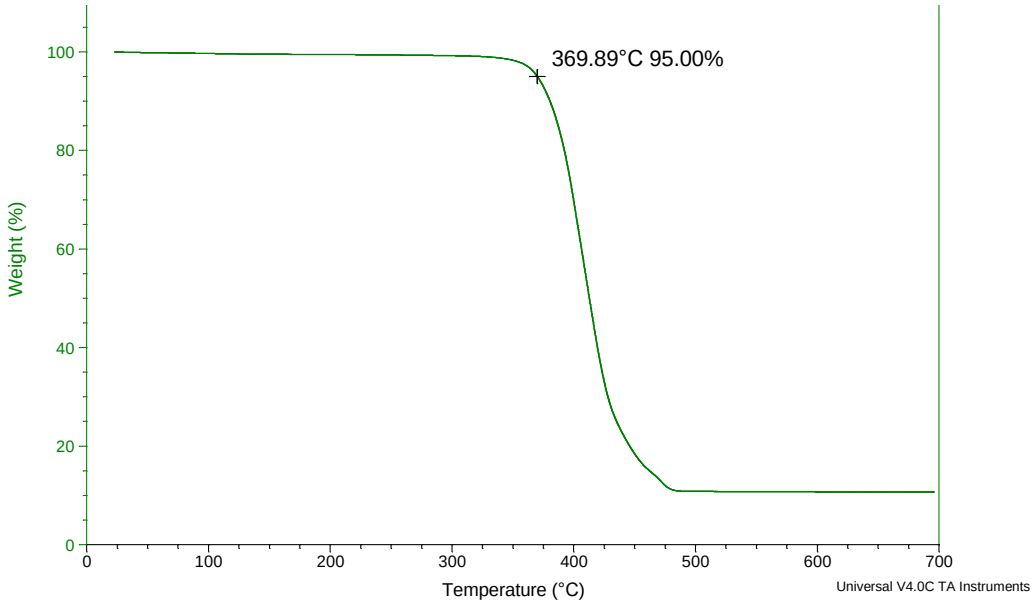

Figure S4. TGA thermogram of PV_C_6/C_{10}.

PV_C_{10}

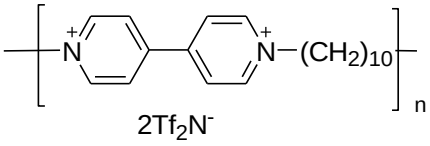

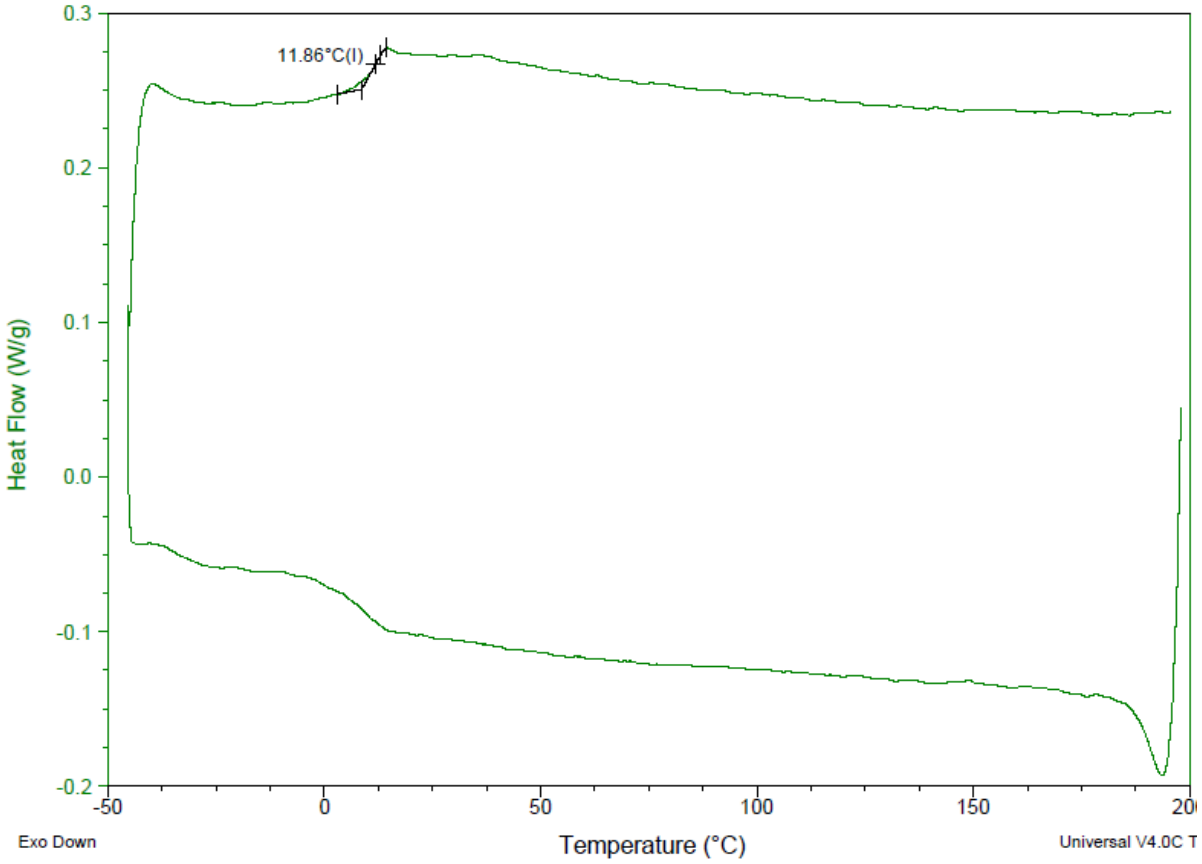

Figure S5. DSC thermogram of PV_C_{10}.

PV_C_6/C_{10}

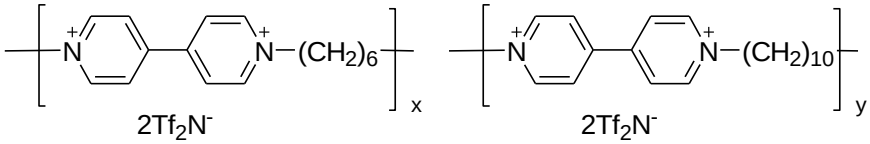

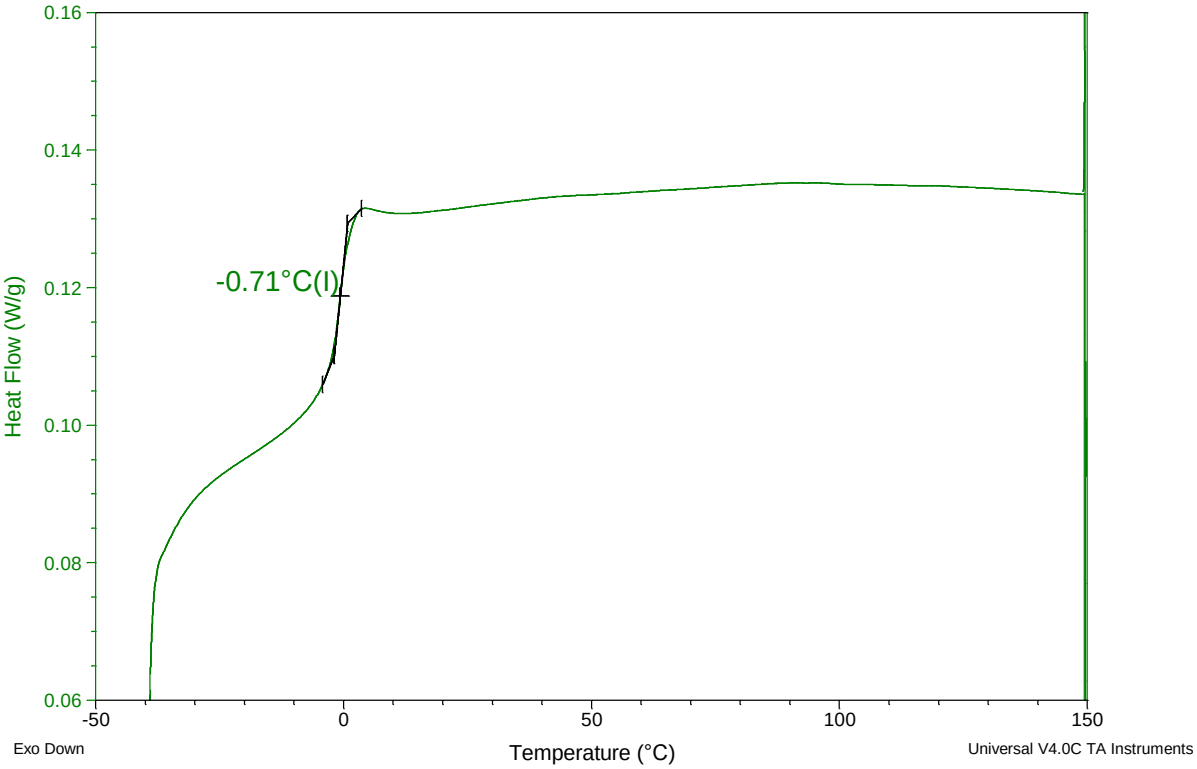

Figure S6. DSC thermogram of PV_C_6/C_{10}.

1:1 molar mixture of **PV_C$_6$** and **PV_C$_{10}$**

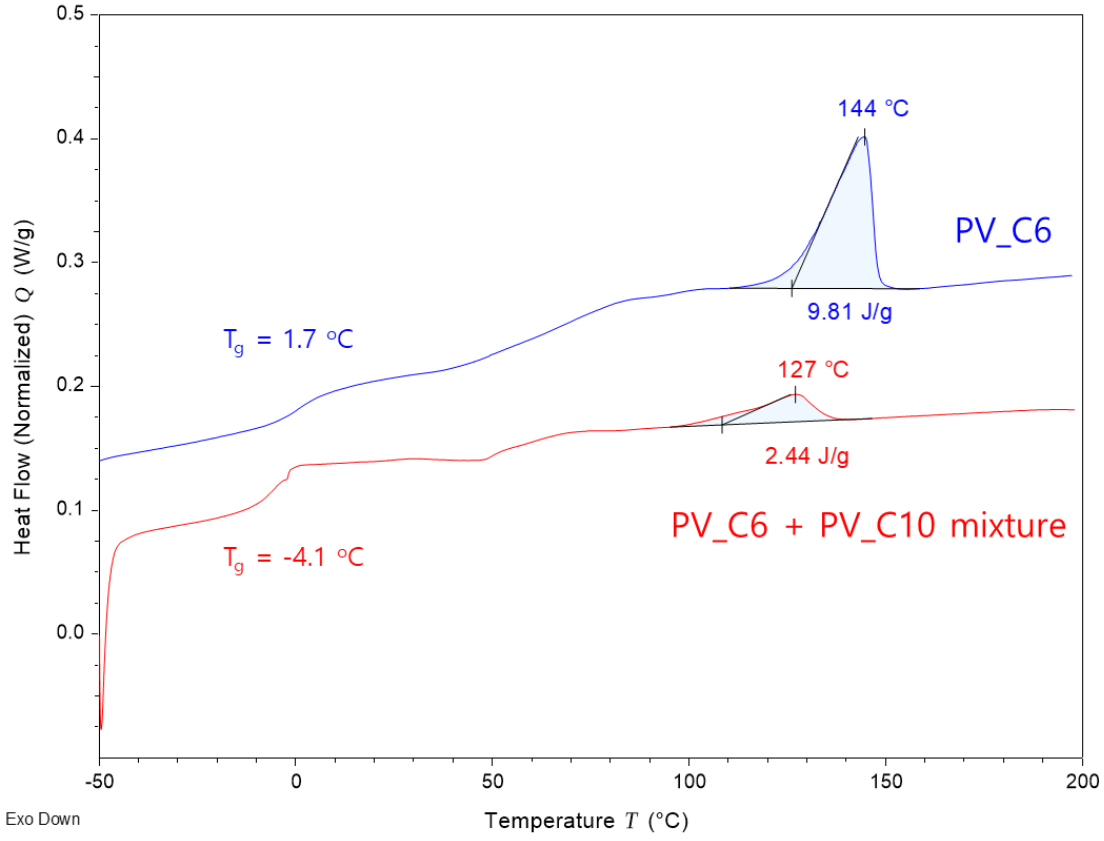

Figure S7. DSC themogram of **PV_C$_6$** (blue curve) and a 1:1 molar mixture of **PV_C$_6$** and **PV_C$_{10}$** (**PV_C$_6$** + **PV_C$_{10}$** mixture, red curve)..

18C6

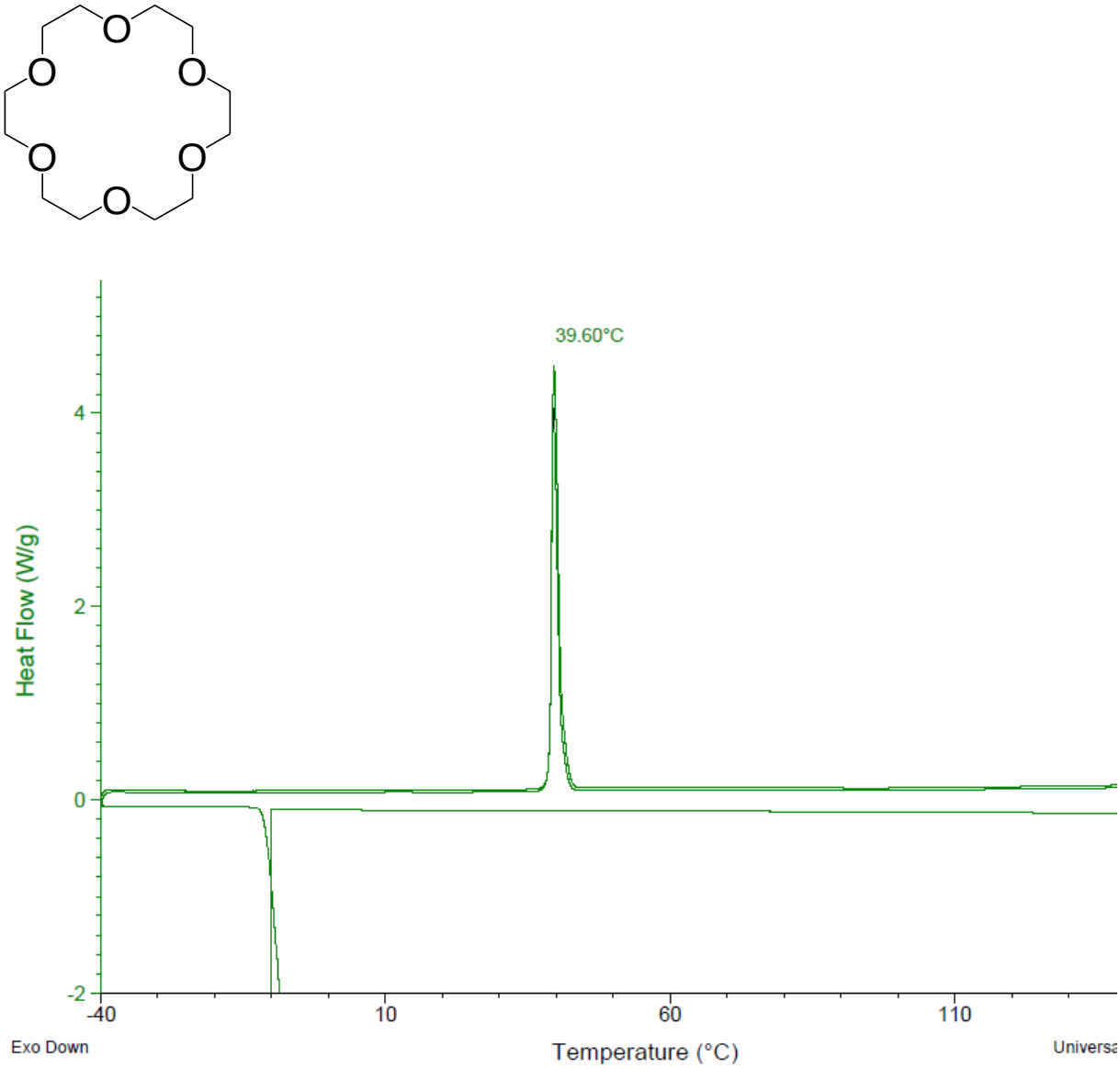

Figure S8. DSC thermogram of 18C6.

PV_C_6/C_{10} + 18C6

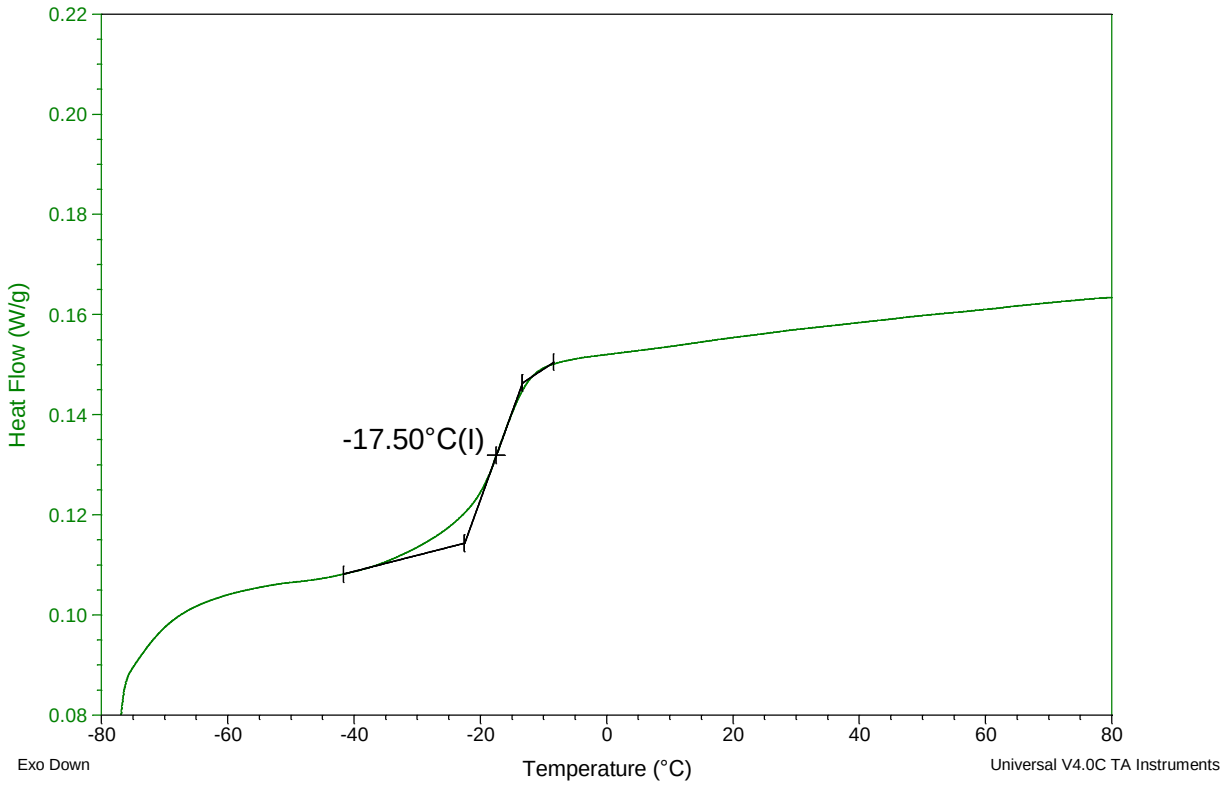

Figure S9 DSC thermogram of PV_C_6/C_{10} + 18C6.

PV_C_6/C_{10} + PEGDME

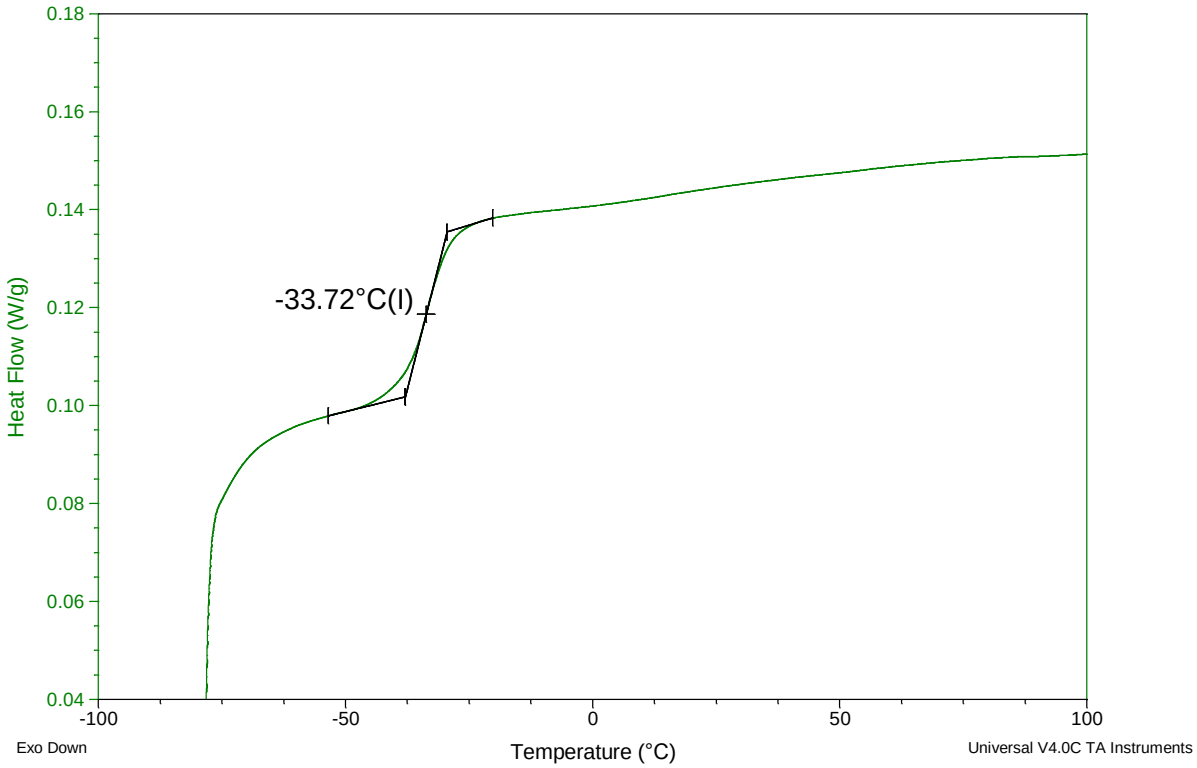

Figure S10. DSC thermogram of PV_C_6/C_{10} + PEGDME.

PV_C_6/C_{10} + 30C10

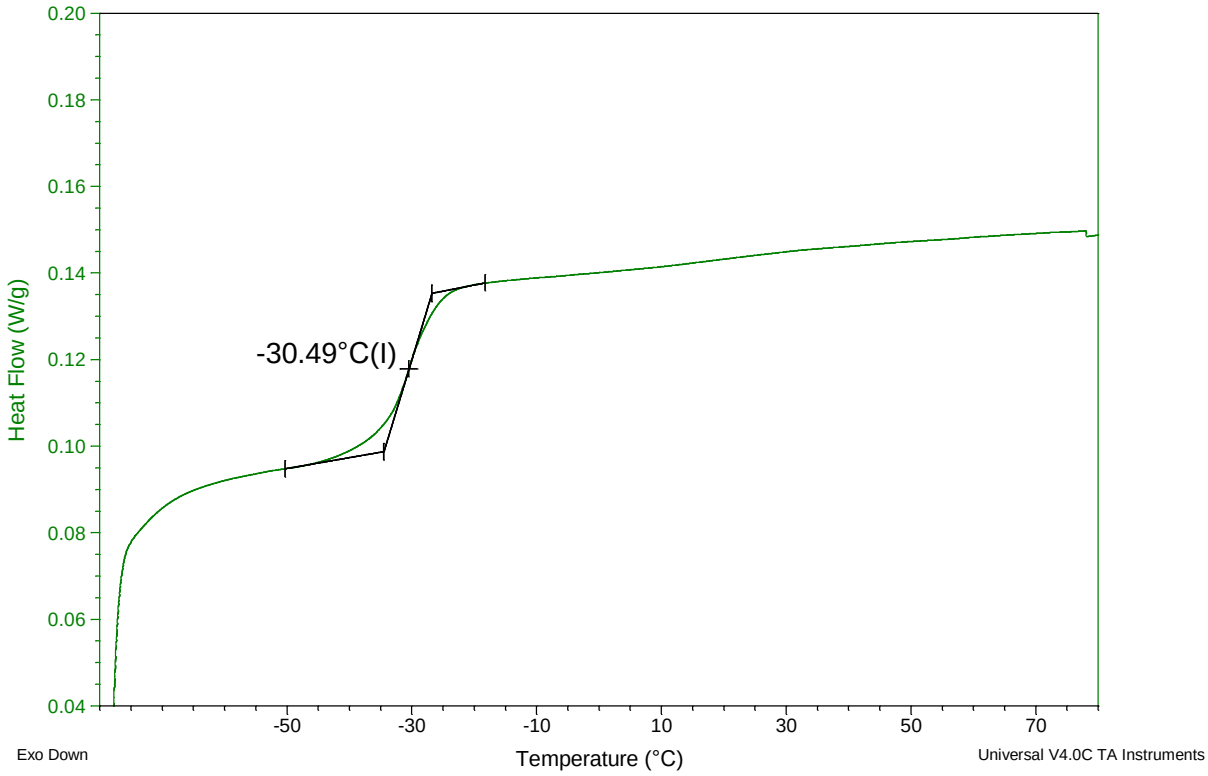

Figure S11. DSC thermogram of PV_C_6/C_{10} + 30C10.

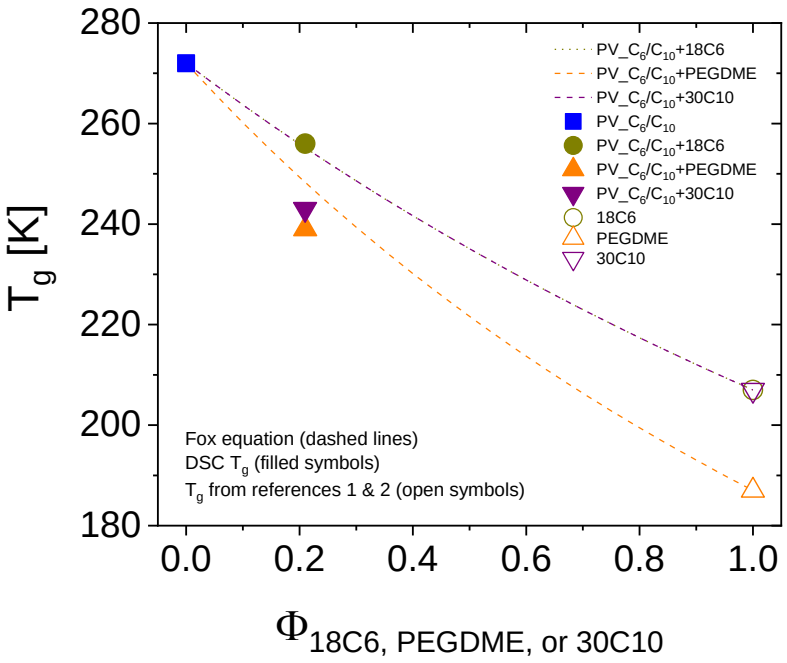

Figure S12. Compositional variation $\Phi_{18C6,\ PEGDME,\ or\ 30C10}$ in the glass transition temperature T_g (filled symbols) for PV_C_6/C_{10} and its mixtures with 18C6, PEGDME, or 30C10, where $\Phi_{18C6,\ PEGDME,\ or\ 30C10}$ is the weight fraction of 18C6, PEGDME, or 30C10. The dashed lines are the Fox equation, using the literature T_g values of 18C6 (T_g = 207 K),[1] PEGDME (T_g = 187 K),[2] and 30C6 (T_g = 207 K)[1] (open symbols).

The effect of the polyether type on the plasticized blend T_gs was compared to predictions from the Fox equation (dashed lines in Figure S12):

$$\frac{1}{T_g} = \frac{\Phi_1}{T_{g1}} + \frac{\Phi_2}{T_{g2}} \qquad \text{(S1)}$$

where T_{g1} = 272 K of **PV_C6/C10**, determined by DSC, T_{g2} = 207 K for 18C6,[1] 187 K for PEGDME,[2] and 207 K for 30C10,[1] from the literature,[1,2] and Φ_1 and Φ_2 are the weight fractions of the two components for the blends. The Fox prediction for **PV_C6/C10**+18C6 (dark yellow dotted line in Figure S12) is close to the observed DSC T_g (dark yellow circle filled symbol), whereas both **PV_C6/C10**+PEGDME and **PV_C6/C10**+30C10 display large negative T_g deviations from the Fox equation. This probably reflects specific interactions or excess free volume formation upon mixing **PV_C6/C10** with PEGDME or 30C10. Therefore, incorporation of PEGDME or 30C10 into **PV_C6/C10** (having higher T_g due to viologen-Tf_2N ion aggregation) allows the guest polyethers to solvate the host viologens and discourage the ion aggregates, thereby decreasing T_g.

Sample Preparation for Dielectric Relaxation Spectroscopy Measurements. The measurements of ionic conductivity and segmental relaxations were conducted on samples that were prepared by allowing them to flow to cover a 30 mm diameter freshly polished brass electrode. To control the sample thickness at 50 μm, two silica spacers were placed on top of the sample after it flowed to cover the bottom electrode. A 10 mm diameter freshly polished brass electrode was then placed on top, and gravity formed a 50 μm parallel plate capacitor cell as the extra sample was squeezed away (with precise thickness verified after dielectric measurements were complete). The capacitor cells, where samples were sandwiched between the two electrodes, were placed in a Novocontrol GmBH Concept 40 broadband dielectric spectrometer, combined with a Quatro Cryosystem as a high-quality temperature control system with vacuum-isolated cryostat and nitrogen lines. Each sample was then annealed in the Quatro Cryosystem sample chamber at 393 K in a heated stream of nitrogen for 1 h prior to the measurements to remove any water acquired during sample loading. The complex dielectric permittivity was measured using an AC voltage amplitude of 0.1 V in a frequency range from 10 MHz to 0.1 Hz for all experiments.

Electrode Polarization Analysis. A physical model of electrode polarization (EP) makes it possible to separate ionic conductivity into the number density of simultaneously conducting ions p and their mobility μ, since $\sigma_{DC} = ep\mu$ with e the elementary charge.[2–6] Electrode polarization occurs at low frequencies, where the transporting ions have sufficient time to polarize at the blocking electrodes during the cycle. That polarization manifests itself in (1) an increase in the effective capacitance of the cell (increasing the apparent dielectric constant) and (2) a decrease in the in-phase part of the conductivity, as the polarizing ions reduce the field experienced by the transporting ions (see Figure S13). The natural time scale for conduction is the time when counterion motion starts to become diffusive

$$\tau_\sigma \equiv \frac{\varepsilon_s \varepsilon_0}{\sigma_{DC}} \tag{S1}$$

wherein ε_s is the measured static relative permittivity of the sample before EP and ε_0 is the permittivity of vacuum. At low frequencies the conducting ions start to polarize at the electrodes and fully polarize at the electrode polarization time scale

$$\tau_{EP} \equiv \frac{\varepsilon_{EP} \varepsilon_0}{\sigma_{DC}} \tag{S2}$$

wherein ε_{EP} is the (considerably larger) effective permittivity after the electrode polarization is complete (see Figure S13). The Macdonald and Coelho model[2–4,7] treats electrode polarization as a simple Debye relaxation with loss tangent,

$$\tan\delta = \frac{\omega\tau_{EP}}{1+\omega^2\tau_\sigma\tau_{EP}} \tag{S3}$$

allowing a two-parameter fit (see Figure S13) to determine the electrode polarization time τ_{EP} and the conductivity time τ_σ. The Macdonald and Coelho model then determines the number density of simultaneously conducting ions p and their mobility μ from τ_{EP} and τ_σ

$$p = \frac{1}{\pi l_B L^2}\left(\frac{\tau_{EP}}{\tau_\sigma}\right)^2 \tag{S4}$$

$$\mu = \frac{eL^2\tau_\sigma}{4\tau_{EP}^2 kT} \tag{S5}$$

wherein $l_B \equiv e^2/(4\pi\varepsilon_s\varepsilon_0 kT)$ is the Bjerrum length, L is the spacing between electrodes, k is the Boltzmann constant and T is absolute temperature.

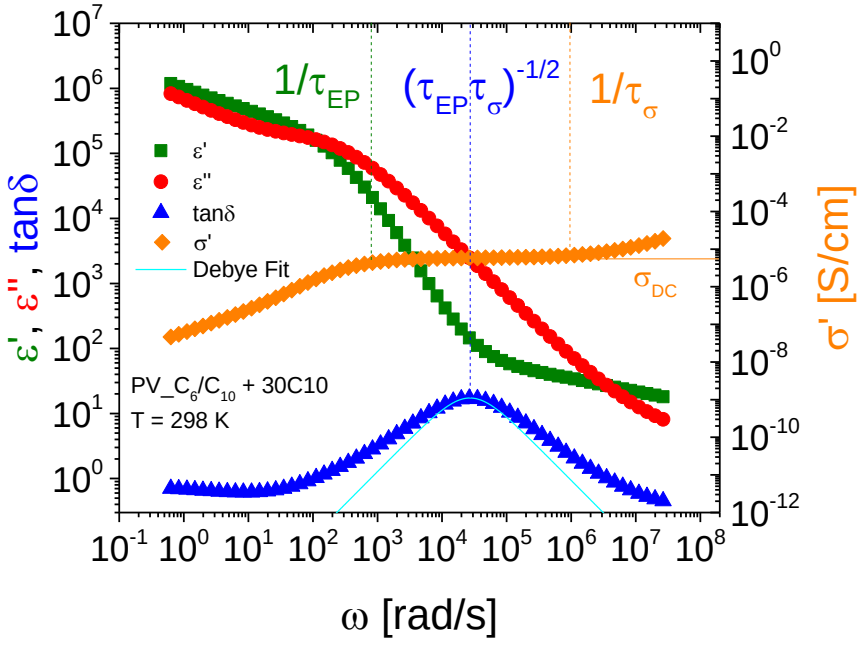

Figure S13. Dielectric response of a blend (PV_C_6/C_{10} + 30C10) to applied AC field at T = 298 K: dielectric constant (ε', green squares), dielectric loss (ε'', red circles), loss tangent ($\tan\delta$, blue triangles), and in-phase part of conductivity (σ', orange diamonds). The peak of the loss tangent gives the geometric mean of the time scales of conductivity and electrode polarization [$(\tau_{EP}\tau_{\sigma})^{1/2}$, dashed lines], then determining the number density of simultaneously conducting ions p and their mobility μ.

MWS Interfacial Polarization

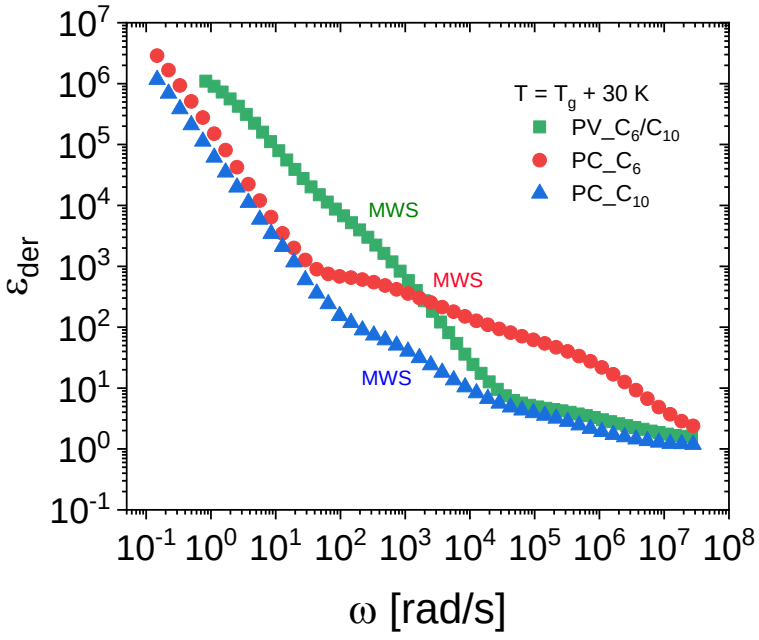

Figure S14. Angular frequency dependence of dielectric derivative spectra $\varepsilon_{der}(\omega)$ for **PV_C6/C10**, **PV_C6**, and **PV_C10** at T_g + 30 K.

Relaxation Strength.

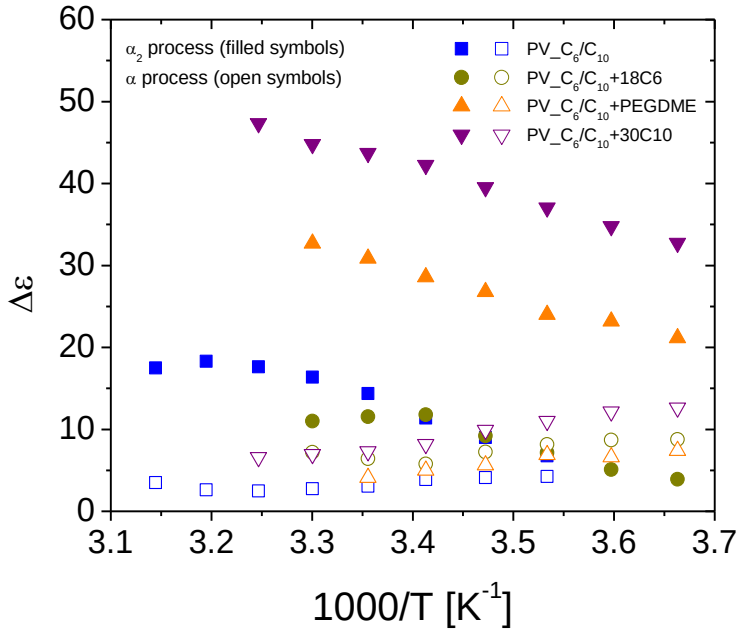

Figure S15. Temperature dependence of relaxation strengths $\Delta\varepsilon$ of the α_2 (filled symbols) and α (open symbols) processes.

Static Dielectric Constant.

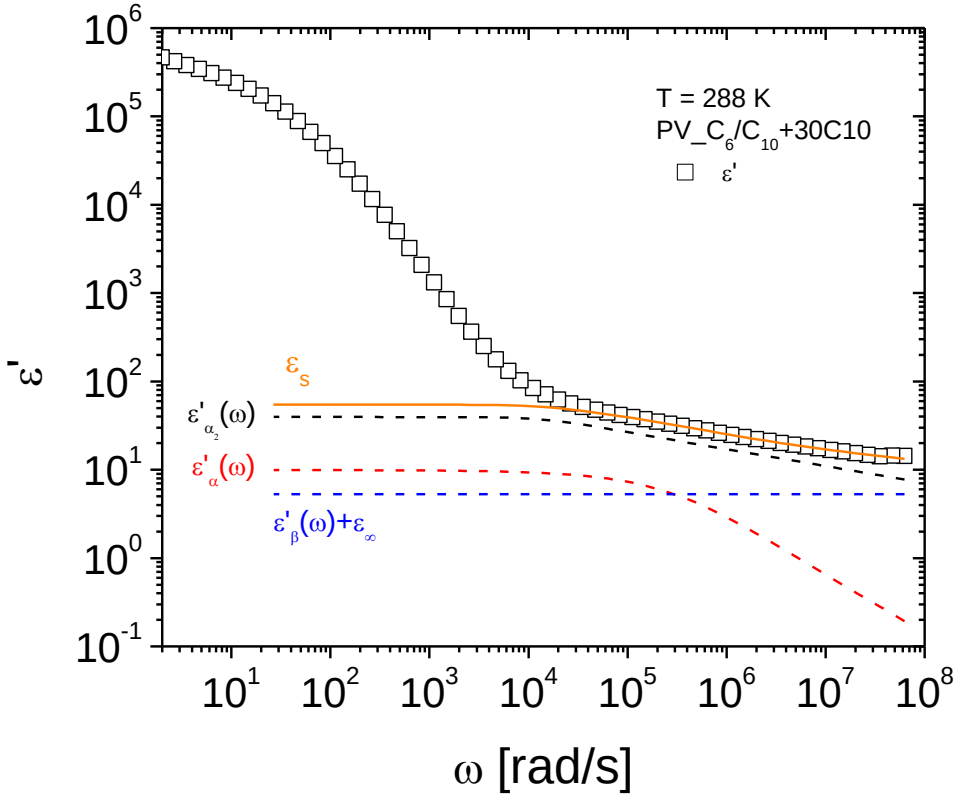

Figure S16. Dielectric permittivity $\varepsilon'(\omega)$ of the PV blend with 30C10 (PV_C_6/C_{10} + 30C10) at 288 K. $\varepsilon'(\omega)$ is decomposed into frequency-dependent contributions from ionic orientational polarization [$\varepsilon'_{\alpha_2}(\omega)$: black dashed line], dipolar orientational polarization [$\varepsilon'_{\alpha}(\omega)$: red dashed line), and the sum of the local dipolar orientational polarization and high-frequency dielectric constant [$\varepsilon'_{\beta}(\omega)+\varepsilon_{\infty}$: blue dashed line], which is the difference between $\varepsilon'(\omega)$ and $\varepsilon'_{\alpha_2}(\omega)+\varepsilon'_{\alpha}(\omega)$ at high frequency $\{\varepsilon'(\omega)-[\varepsilon'_{\alpha_2}(\omega)+\varepsilon'_{\alpha}(\omega)]\}$.[8] The orange solid line indicates the static dielectric constant ε_s.

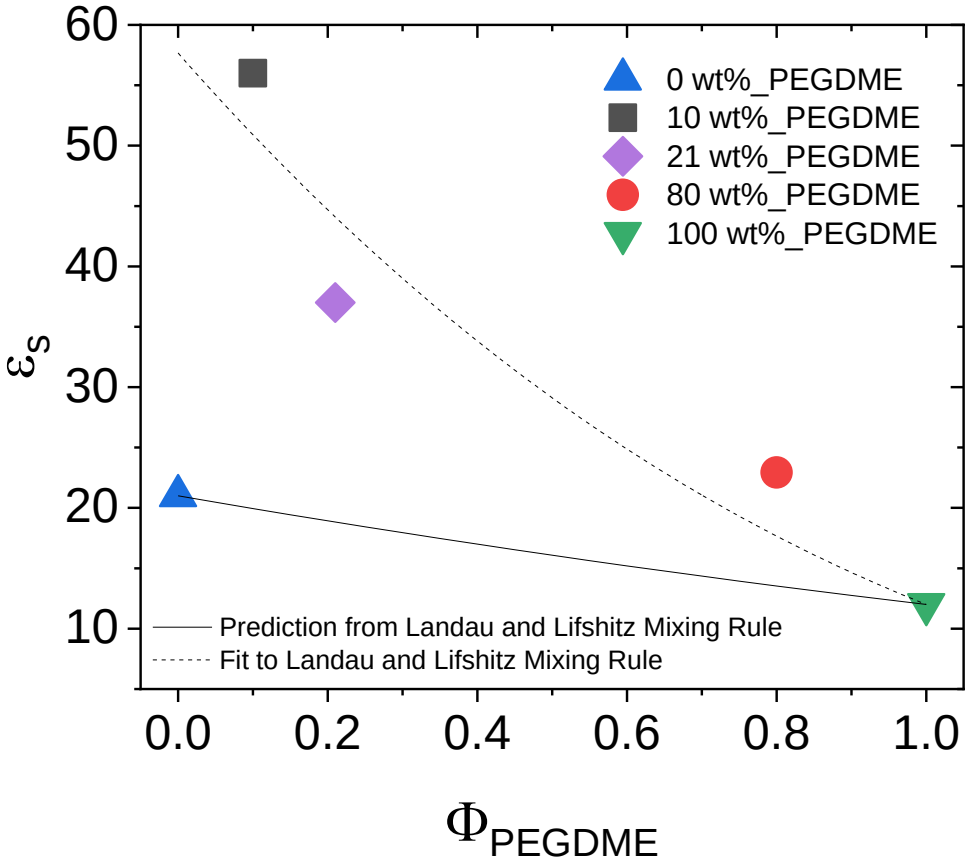

Figure S17. Compositional variation in the static dielectric constant ε_s at room temperature for the neat **PV_C6/C10**, its mixtures with PEGDME, and the neat PEGDME. The solid and dashed curves indicate the prediction from Landau and Lifshitz's mixing rule (eq S6) and a fit to Landau and Lifshitz's mixing rule, respectively.

The composition dependence of the static dielectric constant for the neat **PV_C6/C10**, its mixtures with PEGDME, and the neat PEGDME was compared with the prediction from the Landau and Lifshitz's dielectric mixing rule (see solid curve in Figure S17):

$$(\varepsilon_s^{\text{mix}})^{1/3} = (1-\Phi_{\text{PE}})(\varepsilon_s^{\text{PV}})^{1/3} + \Phi_{\text{PE}}(\varepsilon_s^{\text{PE}})^{1/3} \quad \text{(S6)}$$

where $\varepsilon_s^{\text{mix}}$, $\varepsilon_s^{\text{PV}} = 21$, and $\varepsilon_s^{\text{PE}} \sim 12$ are the static dielectric constant of the PV mixture (**PV_C$_6$/C$_{10}$** + PEGDME), neat PV, and PEGDME, respectively, and Φ_{PE} is the weight fraction of PEGDME. The static dielectric constant at lower PEGDME concentrations is far above Landau and Lifshitz's prediction, and increasing PEGDME content leads to a decrease in the static dielectric constant of the mixtures, but the ε_s value is still higher than the predicted one from eq S6 (solid curve in Figure S17). This presumably indicates that the **PV_C$_6$/C$_{10}$** blends with the plasticizer have additional ion dipoles induced by plasticizers, for example, Tf_2N^- counteranions being further away from the EO moieties by the plasticizer complexation with the viologen cations, creating more separated ion pairs and thereby enhancing the dipole moment and static dielectric constant. This complexation cannot be predicted from the dielectric constant values of the pure PV (where most of ion dipoles remain contact state) and plasticizer using the Landau and Lifshitz's dielectric mixing rule.

Table S1. Blend Compositions of **PV_C$_6$/C$_{10}$** and Polyethers

Blend Entry	**PV_C$_6$/C$_{10}$**	Polyethers	Target[a] [EO]/[PQ]
PV_C$_6$/C$_{10}$ + 18C6	0.7176 g (0.866 mmol PQ)	18C6 0.1907 g (0.722 mmol)	5.0
PV_C$_6$/C$_{10}$ + 30C10	0.7169 g (0.865 mmol PQ)	30C10 0.1905 g (0.433 mmol)	5.0
PV_C$_6$/C$_{10}$ + PEGDME	0.7183 g (0.867 mmol PQ)	PEGDME M_n = 1000 0.1910 g (0.191 mmol)	5.0

[a] The ratio 1:5 (viologen [PQ]:ethyleneoxy [EO]) is originally from the 2:1 molar ratio of viologen:30C10. The molar amount of 30C10 is set as a half of the PV unit. When the binding constant is high enough to realize that all 30C10 rings can be complexed to the viologen units, we do not want any residual crown molecules acting as a plasticizer in the mixture system. For 18C6, the 1:5 viologen:ethyleneoxy ratio means the actual molar ratio 1:0.83. Also we do not want to add more 18C6 molecules than the PV units.

Table S2. Fitting Parameters of the VFT and Arrhenius Equations for DC conductivity, Eq 1

sample	DC conductivity				
	VFT ($T > T_g$)			Arrhenius ($T < T_g$)	
	σ_∞ (S/cm)	D	T_0 (K)	σ_∞ (S/cm)	E_a^σ (kJ/mol)
PV_C$_6$	2.14	10.0	203	-	-
PV_C$_{10}$	0.68	4.2	239	3.4×10^7	95
PV_C$_6$/C$_{10}$	0.50	4.0	237	8.5×10^{15}	140

References

(1) Gibson, H. W.; Marand, H. Polyrotaxanes: Molecular Composites Derived by Physical Linkage of Cyclic and Linear Species. *Adv. Mater.* **1993**, *5*, 11–21.

(2) Kang, M. -S.; Kim, Y. J.; Won, J.; Kang, Y. S. Roles of Terminal Groups of Oligomer Electrolytes in Determining Photovoltaic Performances of Dye-Sensitized Solar Cells. *Chem. Commun.* **2005**, *0*, 2686–2688.

(3) Macdonald, J. R. Theory of AC Space-Charge Polarization Effects in Photoconductors, Semiconductors, and Electrolytes. *Phys. Rev.* **1953**, *92*, 4–17.

(4) Coelho, R. Sur La Relaxation d'une Charge d'espace. *Rev. Phys. Appl.* **1983**, *18*, 137–146.

(5) Klein, R. J.; Zhang, S. H.; Dou, S.; Jones, B. H.; Colby, R. H.; Runt, J. Modeling Electrode Polarization in Dielectric Spectroscopy: Ion Mobility and Mobile Ion Concentration of Single-Ion Polymer Electrolytes. *J. Chem. Phys.* **2006**, *124*, 144903.

(6) Fragiadakis, D.; Dou, S.; Colby, R. H.; Runt, J. Molecular Mobility and Li^+ Conduction in Polyester Copolymer Ionomers Based on Poly(ethylene oxide). *J. Chem. Phys.* **2009**, *130*, 64907.

(7) Choi, U. H.; Lee, M.; Wang, S.; Liu, W.; Winey, K. I.; Gibson, H. W.; Colby, R. H. Ionic Conduction and Dielectric Response of Poly(imidazolium acrylate) Ionomers. *Macromolecules* **2012**, *45*, 3974–3985.

(8) Coelho, R. *Physics of Dielectrics for the Engineer*; Elsevier: New York, 1979.

(9) Choi, U. H.; Mittal, A.; Price, T. L.; Gibson, H. W.; Runt, J.; Colby, R. H. Polymerized Ionic Liquids with Enhanced Static Dielectric Constants. *Macromolecules* **2013**, *46*, 1175–1186.